Energy Conversion and Management 152 (2017) 166–175

Contents lists available at ScienceDirect

Energy Conversion and Management

journal homepage: www.elsevier.com/locate/enconman

An out-of-plane rotational energy harvesting system for low frequency environments

M. Febbo[a,*], S.P. Machado[b], C.D. Gatti[b], J.M. Ramirez[b]

[a] Instituto de Física del Sur (IFISUR) and Departamento de Física, Universidad Nacional del Sur (UNS), CONICET, Av Alem 1253, 8000 Bahía Blanca, Argentina
[b] Grupo de Investigación en Multifísica aplicada, Universidad Tecnológica Nacional FRBB and CONICET, 11 de Abril 461, 8000 Bahía Blanca, Argentina

ARTICLE INFO

Keywords:
Low frequency
Rotational energy haversting device
Wind turbines

ABSTRACT

We present a novel design of a rotational power scavenging system as an alternative to cantilever beams attached to a hub. The device is meant to provide energy to wireless autonomous monitoring systems in low frequency environments such as wind turbines of 30 kW with rotational speeds of between 50 and 150 rpm. These characteristics define the bandwidth of the rotational energy harvesting system (REH) and its physical dimensions. A versatile geometric configuration with two elastic beams and two heavy masses joined by a spring is proposed. A piezoelectric sheet is mounted on the primary beam while the REH is placed on a rotating hub with the gravitational force acting as a periodic source. This kind of double-beam system offers the possibility to modify the vibration characteristics of the harvester for achieving high power density. An analytical framework using the Lagrangian formulation is derived to describe the motion of the system and the voltage output as a function of rotation speed. Several sets of experiments were performed to characterize the system and to validate the assumed hypothesis. In the experimental setup, a wireless data acquisition system based on Arduino technology was implemented to avoid slip-ring mechanisms. The results show very good agreement between the theoretical and experimental tests. Moreover, the output power of a simple harvesting circuit, which serves as an energy storage device, yields values ranging 26–105 μW over the whole frequency range. This allows us to use the proposed device for the designed purpose, taking into account the power requirements of commercially available wireless transmitter systems.

1. Introduction

The condition monitoring of structures and rotating machines is highly desirable to improve the health, safety and failure predictability of civil and industrial systems. In this sense, data transmission and sensors are essential elements. Between wired and wireless communication systems, wireless sensing is more appropriate for sensory data acquisition in applications involving rotary motion. The design of piezoelectric energy scavenging systems for low frequencies (< 100 Hz) and low accelerations (< 1 g) are subjects of current research efforts, mainly because the amplitude of environmental vibration sources is below 0.3 g (or 3 m/s^2) and 30 Hz [1,2].

Vibrating energy harvesting (VEH) systems have been developed largely in this sense, considering different mechanical designs, fields of application and transduction mechanisms [3–6]. Other mechanisms used in energy harvesting include solar [7], thermal [8], electromagnetic [2] and triboelectric devices for exploiting renewable energy sources as well [9]. However, energy harvesting from rotational motion has been much less investigated in the literature even though there is a large subset of civil or industrial scenarios where rotational kinetic energy is available, for example gas and wind turbines, rotating machines, car tires, wheels, shafts, fans, among others. Thus, powering condition-monitoring systems with rotational energy harvesters sounds promising and attainable.

There are several facts that make harvesting energy from rotations distinct from harvesting energy from vibrations. Firstly, if the harvesting device is properly oriented, Earth's gravity can act as a source of periodic excitation with the frequency of the rotational speed. Secondly, the centrifugal force, which grows with the square of the rotational speed, induces large constant body forces, while the system is rotating. These issues may represent singular benefits to the mechanical designer to improve energy harvest and adapt a mechanism to scavenge energy in low frequency and low acceleration environments. For example, a passive tuning scheme can be implemented with the centrifugal force acting as an axial force that can change the stiffness of a cantilever beam piezoelectric system. This type of approach has been successfully used by Leland and Wright [10] and Eichhorn et al. [11], who applied a compressive axial preload to a vibration energy scavenger to adjust its resonance frequency.

* Corresponding author.
E-mail address: mfebbo@uns.edu.ar (M. Febbo).

http://dx.doi.org/10.1016/j.enconman.2017.09.042
Received 19 June 2017; Received in revised form 28 August 2017; Accepted 16 September 2017

Nomenclature

w	transverse elastic displacements (m)
u	axial elastic displacements (m)
t	time (s)
e_x	unit vector in the x direction
e_z	unit vector in the z direction
H_n	Heaviside function
ϕ_j	j^{th} normalized mode shapes functions
q_j	j^{th} mode of the generalized coordinate
K_j	j^{th} modal stiffness
χ_j	j^{th} equivalent "modal" radius
Γ_j	j^{th} modal excitation
ω_j	j^{th} modal natural frequency (rad/s)
ξ_j	j^{th} modal damping
ϑ_j	j^{th} piezoelectric coupling of mode
$\dot{\theta} = \Omega$	rotating frequency (rad/s)
R	position of an infinitesimal segment on the beam in the rotating coordinates (m)
r	distance from the axis of rotation to the beams (m)
r_1	distance from the axis of rotation to the beam#1 (m)
r_2	distance from the axis of rotation to the beam#2 (m)
d_1	offset distance of the tip mass#1 (m)
d_2	offset distance of the tip mass#2 (m)
M_1	heavy mass#1 (kg)
M_2	heavy mass#2 (kg)
I_{T1}	moment of inertia of the tip mass#1 (m^4)
I_{T2}	moment of inertia of the tip mass#2 (m^4)
k	linear spring stiffness (N/m)
n	number of beam sections (n = 1, 2 and 3)
L_n	length of each section (m)
EI_n	flexural beam rigidity for each section (N m^2)
ρA_n	area density for each section (kg/m)
t_n	thickness of each beam's section (m)
b_n	width of each beam's section (m)
c	linear damping coefficient (Ns/m)
g	gravity (m/seg^2)
C_p	internal capacitance of the piezoceramic (nF)
v	voltage drop in the piezoelectric (V)
V_{oc}	open-circuit voltage (V)
J_p	electromechanical coupling coefficient (Npm/V)
d_{31}	piezoelectric constant (pm/V)
R	resistive load (Ohm)
P	power (W)
t_p	piezoelectric thickness (m)
b_p	piezoelectric width (m)
a	distance from the neutral axis to the bottom piezoelectric layer (m)
E_p	piezoelectric Young's modulus (N/m^2)
V	voltage amplitude (V)

A common practice in the design of VEH devices to maximize power is matching the resonant frequency of the harvester to the excitation frequency. This approach appears to be applicable also to rotational devices. However, a main drawback of this methodology is that the physical dimensions of the devices (especially at low frequencies) are such that it is impossible to fit them given the size and weight limitations of practical applications. In rotating devices such as car-tires, wheels or shafts, the reduced availability of space is crucial and determines the actual design of the harvesting device. In the following paragraphs, a brief survey of the literature on rotational energy harvesting (REH) devices is presented. Manla et al. [12] proposed a system of power generation from rotating vehicle wheels using a piezoelectric generator and a ball bearing. The system is designed to be a tire pressure monitoring system (TPMS). The ball impacts the piezoelectric transducer inside a tube by means of the centrifugal force. Experiments showed that the device can produce 4 mW of electrical power at 800 rpm in a volume of 2 cm^3. They also demonstrated that increasing both the tube length and the mass of the ball bearing increases the output power. Also Zheng et al. [13] developed a TPMS based on a novel asymmetric air-spaced piezoelectric cantilever. They reported that the device has several desirable advantages. Firstly, the voltage generated is increased due to the much larger distance between the piezo layers and the neutral plane; and secondly, the asymmetric structure makes the device more robust since the piezo layer is operating in the compression mode. The prototype was capable of generating 47 μW with a 21.6 gr. proof mass at a driving speed of 80 km/h. More recently, Roundy and Tola [14] presented an energy harvester using the dynamics of an offset pendulum along with a nonlinear bistable restoring spring to improve the operational bandwidth of the system. Depending on the speed of the rotating environment, the system can act as a bistable oscillator, a monostable stiffening oscillator, or linear oscillator. Simulation and experimental tests showed that the prototype generator is capable of directly powering an RF transmission system every 60 s or less over a speed range of 10–155 km/h. With the aim to powering a TPMS, Manla et al. [15] developed an off-axis piezoelectric device consisting of pre-stresses piezoelectric beams and a magnet, which is capable of generating energy in a large range of rotational speeds due to the implementation of a levitating magnet that generates nonlinear magnetic over a wide range of centrifugal forces. The prototype occupies a volume of approximately 17.74 cm^3 and generates an output power ranging from 0.2 to 3.5 μW when the rotating speed changes from 180 rpm to 330 rpm.

A passive self-tuning REH device was presented by Gu and Livermore [16]. Their harvester comprises a radially oriented beam mounted at a distance r from the axis of rotation. As the rotational speed varies, the corresponding tension due to centrifugal force on the beam adjusts the beam's resonant frequency so that the harvester always works at or near its resonant frequency. In this way, and under a proper design, the resonant frequency of the harvester can match the frequency of the rotation over a wide frequency range, significantly improving its performance compared with an untuned REH. The same authors also presented an impact-based REH that also works as a self-tuning device with an optimized design [17]. The system comprises two beams: a rigid piezoelectric generating beam and a narrow, flexible driving beam with a tip mass at the end. The mass impacts the generating beam repeatedly under the influence of gravity to drive generation, while the centrifugal force from the rotation modifies the resonant frequency of the flexible driving beam and the frequency response of the harvester. Thus the generation is improved due to the self-tuning mechanism. As a result, the system is capable of generating a power density of 30.8 μW/cm^3 over a wide frequency range. Khameneifar et al. [18,19] proposed and tested a REH system consisting of a rotating piezoelectric cantilever beam with a tip mass mounted on a hub. The gravitational force generates mechanical excitation while the hub is in rotary motion. Expressions for the optimum load resistance and maximum power were obtained and experimentally validated using PDVF and PZT transducers. A maximum power of 6.4 mW at a rotational speed of 1320 rpm been achieved with a 0.25 cm^3 PZT device. This is about 44 times higher than when a PVDF film is used. Thus, their proposal could be used as a power generator for a wireless communication system. For low frequency (< 1 Hz) and low size (< 10 cm), a hybrid electromagnetic-tribolectric nanogenerator consisting of four units of freestanding triboelectric nano generators (TENG) and four electromagnetic generators (EMG) [9] can be used as a self-powered sensor for road traffic monitoring. With an optimization of the geometry of the electromagnetic component and with the combination of

TENG and EMG, Askari et al. [9] showed that the proposed device is capable of the power and voltage generation even with very small displacements and low frequencies. Moreover, depending on the triggering frequency, TENG or EMG dominates the power generation considering different mechanical loads.

More recently, Hsu et al. [20] presented a self-frequency tuning REH consisting of a cantilever beam mounted on a rotating axis, similar to the configuration in [18]. The difference is that, in this case, the numerical results obtained by a commercial software package which implements FEM calculations take into account shear deformation, piezoelectric plate, and the centrifugal force in the piezoelectric beam. The beam is oriented in the radial direction, so that the tensile stress induced by the centrifugal force stiffens the beam to passively tune the resonance frequency. The results show a relatively good power generation, verifying the frequency-tuning, but they fail to predict a precise voltage peak generation. Recently, Guan and Liao [21] reported a very promising generation about 80–800 μW on a REH with a cantilever piezoelectric beam at rotating frequencies of 7–13.5 Hz. Their proposal is based on rotating cantilever beams where the mass center of the rotating beam coincides with the center of rotation. This allows to harness the full drive of the gravitational force and reduce the amplitude of the centrifugal force. The generated high output voltage proved to be enough to power low-power wireless communication nodes.

As for nonlinear effects harnessing, nonlinear magnetic interactions have been proposed to increase the bandwidth of VEHs. The pioneering works of Cottone et al. [22] and Erturk et al. [23] presented some of the first evidence in the use of nonlinear phenomena for this purpose. Cottone et al. [22] studied a piezoelectric inverted pendulum where a small magnet was added on top of the pendulum. The dynamics of the inverted pendulum tip is controlled with the introduction of an external magnet determining the mono-stable or bistable characteristics of the interaction. The results showed that, under stochastic excitation for the bistable potential condition, the harvested power increased between 400% and 600% compared to the monostable case. Erturk et al. [23] presented a ferromagnetic cantilever beam with piezoelectric layers attached to the root of the cantilever, and two permanent magnets located symmetrically near the free end and subjected to harmonic base excitation. The system exhibited a strange attractor motion as a mechanical structure. They reported that this generator yields large-amplitude periodic oscillations for excitations over a frequency range. Comparisons were made against a conventional case without magnetic buckling and the superiority of the piezomagnetoelastic structure as a broadband electric generator was demonstrated. It resulted in a 200% increase in the open-circuit voltage amplitude.

In rotating environments, Ramezampour et al. [24] presented an interesting work. They proposed a frequency up-converting REH acting through the magnetic interaction provided by several magnets placed on a rotating shaft, while passing near a PZT cantilever beam fixed to a base. They theoretically and experimentally demonstrated that by applying an appropriate number of rotating magnets the extracted power can be enhanced even more than ten times.

Our proposal presents the following original contributions:

- An alternative to cantilever beam-type systems for energy harvesting in low frequency rotational environments.
- A versatile geometrical configuration with two elastic beams and two heavy system joined by a spring with the possibility to modify several parameters of the harvester for achieving high power density.
- A wireless data acquisition system based on Arduino technology to avoid slip-ring mechanisms.
- Generation of sufficient DC power to feed low power wireless transmitters.

The paper organization of the paper is as follows. After an introductory section, the REH design is presented and the analytical model describing its dynamics and the electrical output voltage is derived in Sections 2 and 3. Section 4 presents the experimental setup and the experiments conducted to validate the theoretical findings. After a discussion of the advantages of the proposed REH device, some concluding remarks are presented in Section 5.

2. Physical considerations and proposal

The most common REH devices consists of cantilevered beams attached to the axis of a rotating system oriented in such a way that they have centrifugal forces proportional to the beam length [14,17]. These conceptual designs may have the disadvantage that these forces are much larger than the gravitational force, and only small transverse vibrations could be generated. An alternative approach to overcome this problem was reported by Guan and Liao [21] who proposed a system to reduce the amplitude of the centrifugal force. Its central idea is to make it comparable to the gravitational force by approaching the mass center of the rotating beam to the center of rotation in zero gravity. This interesting approach generates an output power in the order of hundreds of microwatts at the expense of having a large seismic (heavy) mass compared to the mass of the piezoelectric beam. To avoid damage to the system from large excursions of the mass, a constrained frame is placed in the system to limit its vibration amplitude. Although this proposal presents a stimulating solution, the system still presents a large natural frequency, far exceeding the operating bandwidth, and the impact of the mass with a frame cannot be properly modeled.

Our alternative for a REH system, which aims to harvest the maximum possible energy from a very low frequency environment (0.8–2.5 Hz) pretends to solve some of the drawbacks mentioned above by means of an innovative mechanical design. Fig. 1 illustrates the proposed device comprising two flexible beams with two heavy masses joined by a spring with a QP16N (Mide Corporation) piezoelectric sheet mounted on one of the beams. All the system is placed on a steel frame supporting the beams, whose longitudinal axes are parallel to the axis of rotation with a variable distance from it. This configuration allows to adjust the system parameters such as the spring constant, the length and width of the beams, the heavy masses or the distance from the rotating axis, not only to have centrifugal forces similar to or below the acceleration of gravity but also to tune the first natural frequency to a value near the excitation frequencies. Moreover, the elastic nature of the (linear) spring between the two masses, allows for a predictable dynamics of the system, thus avoiding unpredictable impacts. The model also gives the possibility to introduce modifications to the geometry of the beams in order to have the first two natural frequencies close to

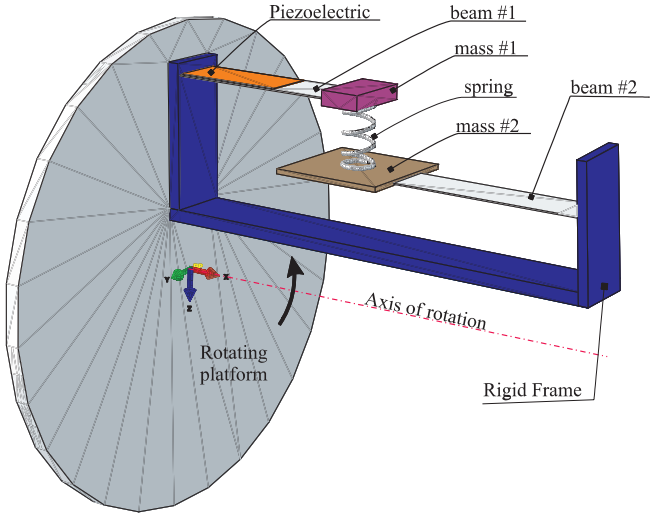

Fig. 1. Schematic view of the rotating energy harvesting system.

each other, improving in this way the generation in a specific (narrow) bandwidth. It is worth mentioning that the selection of a linear spring in this first presentation of the device is for the sake of simplicity in the analysis of the system. However, there is theoretical evidence that selecting a nonlinear spring could improve the harvested energy [22,23,25]. The implementation of a nonlinear spring could be conducted in a future work.

3. Mathematical model

Fig. 1 shows a schematic view of the proposed system, which is connected to a rotating cylindrical hub at a certain distance from the axis. As mentioned above, the axis of rotation is perpendicular to Earth's axis, with gravity acting as an alternating excitation on the REH system for one cycle of rotation. Therefore, the frequency of the excitation force will correspond to the rotating frequency of the hub and the voltage generated in the piezoelectric patch will be a function of the gravitational force caused mainly by the heavy masses and the rotating speed.

Fig. 2 presents the geometric parameters of the REH device. R corresponds to the position of an infinitesimal segment on the beam in the rotating coordinate system, and r is the distance from the axis of rotation to the beams. Therefore, we have

$$R = (r + w)e_x + ue_z \tag{1}$$

where w and u are the transverse and axial elastic displacements respectively, while e_x and e_z are unit vectors in the x and z directions respectively. The velocity of an infinitesimal segment on the structural system is

$$\dot{R} = \frac{dR}{dt} + \dot{\theta} \times R \tag{2}$$

which can be written as

$$\dot{R} = \dot{w}e_x + (r + w)\dot{\theta}e_z \tag{3}$$

In this case the bending motions will not induce significant axial motions, and for that reason they are neglected.

The kinetic energy of the system is

$$T = \frac{1}{2}\rho A \int_0^l \dot{R}^2 \mathrm{d}x + \frac{1}{2}m_T \dot{R}t \cdot \dot{R}t + \frac{1}{2}I_T \dot{w}'^2_{x=L_1+L_2} \tag{4}$$

where l is the length of the structural system, m_T represent the tip masses (M_1 or M_2), I_T is the moment of inertia of the tip (heavy) mass and the velocity of the heavy mass at the free end is

$$\dot{R}t = (\dot{w} + d\dot{w}'_{x=L_1+L_2})e_x + (r + w_{x=L_1+L_2} + dw'_{x=L_1+L_2})\dot{\theta}e_z \tag{5}$$

where d is the length from the tip of the beam to the center of the heavy mass (see Fig. 2). Substituting Eqs. (3) and (5) into Eq. (4):

$$\begin{aligned} T = {} & \frac{1}{2}\rho A \int_0^l [\dot{w}^2 + \dot{\theta}^2(w^2 + r^2 + 2rw)]\mathrm{d}x + \frac{1}{2}m_T(r^2\dot{\theta}^2 + 2r\dot{\theta}^2 w_{x=L_1+L_2} \\ & + \dot{\theta}^2 w^2_{x=L_1+L_2} + \dot{w}^2_{x=L_1+L_2}) + \dot{\theta}^2(2drw'_{x=L_1+L_2} + 2dw_{x=L_1+L_2}w'_{x=L_1+L_2} \\ & + d^2 w'^2_{x=L_1+L_2}) + (2d\dot{w}_{x=L_1+L_2}\dot{w}'_{x=L_1+L_2} + d^2\dot{w}'^2_{x=L_1+L_2}) + \frac{1}{2}I_T\dot{w}'^2_{x=L_1+L_2} \end{aligned} \tag{6}$$

The potential energy of the system can be expressed as

$$\begin{aligned} U = {} & \frac{1}{2}EI\int_0^l w''^2 \mathrm{d}x + g\rho A\int_0^l (r + w)sen\theta dx \\ & + m_T g[(r + w_{x=L_1+L_2} + dw'_{x=L_1+L_2})sen\theta] - \frac{1}{2}J_p v\int_0^l w''\mathrm{d}x \end{aligned} \tag{7}$$

where J_p is the electromechanical coupling coefficient, v is the voltage drop in the piezoelectric, EI is the flexural rigidity which depends on the section of the structural system and g is gravity.

The internal electrical energy in the piezoceramic layer is

$$W_{ie} = \frac{1}{2}J_p v\int_0^l \frac{\partial^2 w}{\partial x^2}\mathrm{d}x + \frac{1}{2}C_p v^2 \tag{8}$$

where C_p is the internal capacitance of the piezoceramic.

The electromechanical Lagrange equations, based on the extended Hamilton's principle can be written as,

$$\begin{aligned} & \frac{d}{dt}\left(\frac{\partial T}{\partial \dot{q}_i}\right) - \frac{\partial T}{\partial q_i} + \frac{\partial U}{\partial q_i} - \frac{\partial W_{ie}}{\partial q_i} = 0 \\ & \frac{d}{dt}\left(\frac{\partial T}{\partial \dot{v}}\right) - \frac{\partial T}{\partial v} + \frac{\partial U}{\partial v} - \frac{\partial W_{ie}}{\partial v} = Q \end{aligned} \tag{9}$$

where Q is the electric charge output of the piezoceramic layer. Other dissipation effects such as mechanical damping will be introduced later as proportional damping.

For the vibration response, we propose a convergent series of eigenfunctions with the following form

$$w(x,t) = \sum_{i=1}^{N} \phi_i(x)q_i(t) \tag{10}$$

where $q_i(t)$ is a time dependent generalized coordinate, and $\phi_i(x)$ are normalized mode shapes functions (eigenfunctions) that satisfy appropriate boundary conditions.

In order to consider the geometric change introduced by the piezoelectric layer and the spring connection, a discontinuous system is proposed to define the orthogonal basis function $\phi_i(x)$

$$\phi_i(x) = \sum_{n=1}^{3} \phi_{i,n}(x)H_n(x) \tag{11}$$

where n is the number of sections and $H_n(x)$ is the Heaviside function to denote the break at $x = L_1$ and at $x = L_2$. For the sake of brevity, the solutions for the three-beam section $\phi_{i,n}(x)$, which satisfy the corresponding compatibility and boundary conditions, are given in Appendix A.

Finally, by applying the Lagrangian formulation to the mechanical

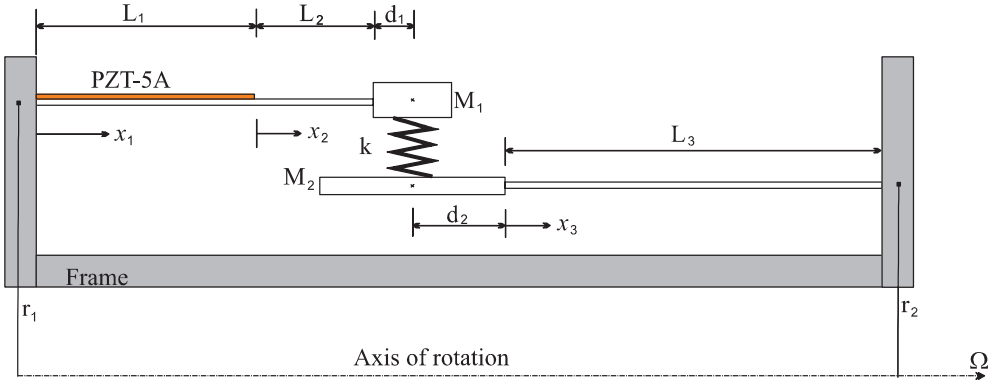

Fig. 2. Geometric parameters of the rotating energy harvesting system.

and electrical degrees of freedom, it is possible to define the governing equations of motion in the following way:

$$\begin{aligned} &\ddot{q} + c\dot{q} + (K - \dot{\theta}^2)q - \dot{\theta}^2\chi + \vartheta v = \Gamma g \sin\theta \\ &C_p\dot{v} + \tfrac{v}{R} + \vartheta\dot{q} = 0 \end{aligned} \tag{12}$$

where c is the mechanical damping, and K, χ, ϑ and Γ are the modal stiffness, an equivalent "modal" radius, piezoelectric modal coupling and the modal excitation produced by rotation, respectively. K, χ, ϑ and Γ are given by

$$\begin{aligned} K_j = {} & EI_1 \int_0^{L_1} \phi''_{j,1}(x)^2 \mathrm{d}x + EI_2 \int_{L_1}^{L_1+L_2} \phi''_{j,2}(x)^2 \mathrm{d}x \\ & + EI_3 \int_{L_1+L_2}^{L_1+L_2+L_3} \phi''_{j,3}(x)^2 \mathrm{d}x + \phi_{i,2}(L_1+L_2)k\left[\phi_{i,2}(L_1+L_2)\right. \\ & \left. -\phi_{i,3}(L_1+L_2)\right] + \phi_{i,3}(L_1+L_2)k\left[\phi_{i,3}(L_1+L_2) - \phi_{i,2}(L_1+L_2)\right] \end{aligned} \tag{13}$$

$$\begin{aligned} \chi_j = {} & r_1\left[\rho A_1 \int_0^{L_1} \phi_{j,1}(x)\mathrm{d}x + \rho A_2 \int_{L_1}^{L_1+L_2} \phi_{j,2}(x)\mathrm{d}x + \phi_{j,2}(L_1+L_2)M_1\right. \\ & + \phi'_{j,2}(L_1+L_2)M_1 d_1\Big] + r_2\left[\rho A_3 \int_{L_1+L_2}^{L_1+L_2+L_3} \phi_{j,3}(x)\mathrm{d}x + \phi_{j,3}(L_1+L_2)M_2\right. \\ & \left. + \phi'_{j,3}(L_1+L_2)M_2 d_2\right] \end{aligned} \tag{14}$$

$$\vartheta_j = d_{31}E_p\frac{b_p}{2}(2a + t_p)\phi'_j(L_1) \tag{15}$$

$$\begin{aligned} \Gamma_j = {} & \rho A_1 \int_0^{L_1} \phi_{j,1}(x)\mathrm{d}x + \rho A_2 \int_{L_1}^{L_1+L_2} \phi_{j,2}(x)\mathrm{d}x + \rho A_3 \int_{L_1+L_2}^{L_1+L_2+L_3} \phi_{j,3}(x)\mathrm{d}x \\ & + \left[\phi_{j,2}(L_1+L_2) + d_1\phi'_{j,2}(L_1+L_2)\right]M_1 + \left[\phi_{j,3}(L_1+L_2)\right. \\ & \left. + d_2\phi'_{j,3}(L_1+L_2)\right]M_2 \end{aligned} \tag{16}$$

where the coefficients EI_n and ρA_n are defined in [26]. In the case of having an external load (such as wind) in addition to the rotational load (multifrequency excitation) one has to analyse first if the magnitude of the external load is comparable to the rotational excitation (1 g = 9.8 m/s^2). If so, Eqs. (12) provide the key to analyse this new dynamical situation. Since these equations are linear, it is possible to apply the superposition principle to solve them. Briefly, it consists in solving Eqs. (12) for each load individually and then adding them up together in order to obtain the new total response.

After solving Eqs. (12), considering a harmonic dependence of all the variables with the rotating frequency $\dot{\theta} = \Omega$, the voltage amplitude is given by:

$$V(\Omega) = \frac{\Gamma_j g \vartheta_j R\Omega}{\sqrt{\left[(\omega_j^2 - \Omega^2) - \Omega^2 - 2C_p R\zeta_j\omega_j\Omega^2\right]^2 + \left[2\Omega\omega_j\zeta_j + R\Omega(\vartheta_j^2 + C_p(\omega_j^2 - \Omega^2) - C_p\Omega^2)\right]^2}} \tag{17}$$

with $\xi_j = \frac{c}{2\omega_j}$ and $\omega_j^2 = K$ the j-th natural frequency of the REH system at 0 rotation speed. This equation expresses the output voltage as a function of rotation speed. It holds from Eq. (17) that the REH system is less stiff than the same REH system in a non-rotational environment. This is imposed by the term $(\omega_j^2 - \Omega^2)$ which sketches the widely known fact that rotation reduces the "natural" frequency of a system by $-\Omega^2$.

In a very low frequency environment, such as the one considered in the present study, it is useful to have a simple expression of Eq. (17). In this sense, an analysis of orders of magnitude allow us to obtain the following linear expression

$$V(\Omega) = \frac{\Gamma_1 g \vartheta_1 R}{\omega_1^2 - 2\Omega^2}\Omega \tag{18}$$

which is the expression for the voltage output in the nearness of the first natural frequency of the REH device. The output power transferred to the resistive load R can be obtained from the voltage amplitude as

$$P = \frac{V^2}{R} \tag{19}$$

It is possible to demonstrate that there exists an optimum resistive load that maximizes this transferred output power, $R^{opt} = \frac{1}{\Omega C_p}$ based on the maximum energy transfer theorem. If we insert this value into Eq. (19), we obtain the value of output power transferred to an optimum resistive load, P^{opt}. This result can also be obtained from the peak open-circuit voltage V_{oc}, making $V(R \to \infty)$ in Eq. (17). This derives in $P^{opt} = V_{oc}^2 \Omega C_p/4$.

With the aim to accumulate the harvested power for a possible use as DC current, a rectifier bridge and an energy storage device are used in the REH device, as shown in Fig. 3.

In this sense, our results provide a direct evaluation of the usable electric power.

4. Experiments and results

The aim of this section is to validate the previous theoretical findings and show the advantages of the proposed REH system. Experimental tests were performed in the following way: an electric motor with a variable speed controller provided the rotational motion of the system, which was rigidly mounted to the hub as observed in Fig. 4. Instead of using a more common slip-ring system, an Arduino board with a Bluetooth connection was used, which connects the collected data to a PC at a rate of 100 samples/s. A first set of experiments was performed with the system connected to a load resistor of 10 KΩ, in order to capture the voltage generation for different rotating frequencies. Such a small value was used for the resistor due to a limitation of the data acquisition system, which presents a maximum possible reading of 5 Vpp (Arduino setting). Table 1 shows the material and geometrical parameters of the REH device. The lengths of the beams were selected considering a reasonable size to mount the REH system in a typical hub of a 30 kW aerogenerator. The heavy masses (M_1 o M_2) were proposed in order to have a ratio of tip displacement to the length of the beams ($L_1 + L_2$, L_3) below 0.1. This allow us to ensure a geometrically linear dynamics for the REH device.

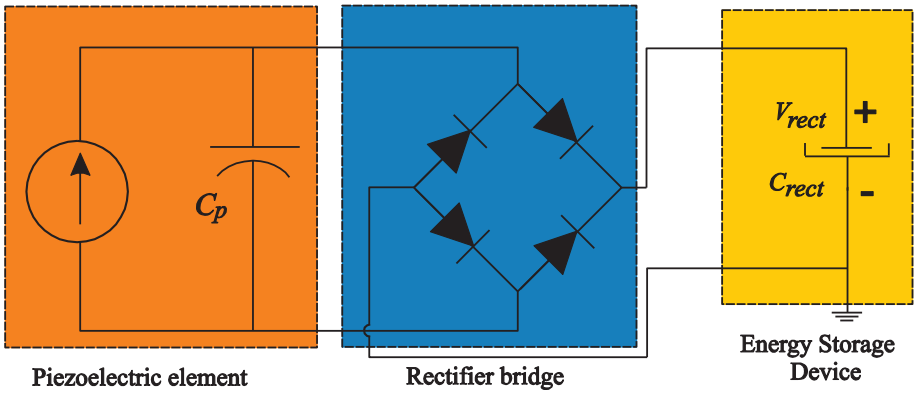

Fig. 3. Schematic representation of a piezoelectric circuit with an AC/DC converter and an energy storage device.

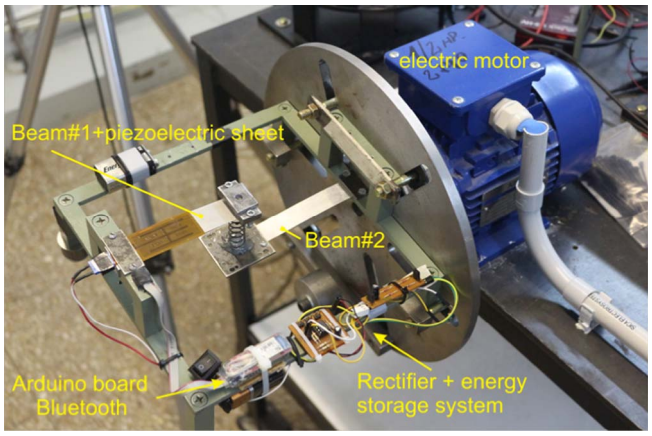

Fig. 4. Photo of the experimental setup used in the experiments. The REH system is attached to an electric motor that induces the rotation of the system.

The experimental output voltage for some selected rotating frequencies (1.173 Hz, 1.956 Hz and 2.594 Hz), corresponding to the desired frequency range of 50–150 rpm, is shown in Fig. 5. It presents a sinusoidal output for various rotating frequencies, according to the periodic excitation due to gravity in the rotating reference frame. As it can be observed, voltage amplitude increases with increasing frequencies. This result holds from Eq. (17) considering increasing rotation speeds far from the first natural frequency of the REH system which is 13.31 Hz, at 0 rotation speed. It must be pointed out that the effect of the softening of the natural frequency due to rotation is small for these low rotating frequencies. In this sense, the first natural frequency decreased to 13.05 Hz for 2.594 Hz.

Fig. 6 and Table 2 present the peak output voltages versus rotating frequency for values between 0.77 and 2.59 Hz (equivalent to 46.2 and 155.4 rpm). A good agreement between both analytical and experimental results is observed. In the case of 0.77 Hz, an output voltage of 0.1027 V is obtained, whereas the system generates 0.4144 V for the maximum considered frequency of 2.59 Hz. A closer analysis of this figure reveals a linear dependence of voltage output on frequency, as it can be predicted by the linearized Eq. (18) (dotted-line).

Having validated our analytical findings, we will now introduce some changes to the system with the aim of increasing energy generation. As stated in the introduction, we propose to increase the flexibility of the secondary beam in order to lower the first frequency of the system. Evidently, other changes such as the modification of the length, width and thickness of the beams, spring stiffness or boundary conditions can be proposed to the same end, but these are left for future studies. From all the possible solutions to increase the flexibility of the secondary beam (beam#2), we select the addition of an extra mass m to obtain a twofold effect: to increase the strain on beam#1 (or beam#2) and therefore the voltage, and to diminish the natural frequency of the REH device. Additionally, this is a very simple modification that can be attempted easily in a real situation. The question that immediately arises is where it will be more beneficial, if it is added to M_1 (beam #1) or M_2 (beam #2). To this end, we carried out numerical and experimental tests. Again, the value of $m = 10.38\ gr$ was selected to ensure a geometrically linear assumption.

Fig. 7 shows the influence of the mass on the first mode shape, as it can be obtained from the numerical solution of Eq. (12), considering a speed rotation of 155 rpm. We can observe that the tip displacement for beam #1 is the same in both cases, regardless of the place where the mass is added (to M_1 (beam #1) or to M_2 (beam #2)). Therefore, it can be deduced that the output voltage will yield the same values.

Then we carried out the experiments to test these numerical predictions. In Fig. 8 and Table 3 we show voltage generation versus frequency for the case where a mass is added to beam #2. For the sake of simplicity, the same range of frequencies as in Fig. 6 is considered. The results present a good agreement between the numerical predictions and the experimental tests. As for voltage generation, the comparison between Figs. 8 and 6 shows larger values of output voltage for this case than those obtained without the addition of mass. For example, 0.438 V was obtained for the maximum rotation speed against 0.414 V obtained in the previous case. In addition, the new natural frequency of the system decreased to 12.24 Hz without rotation, as it was also expected. Finally, a linear dependence of the voltage with frequency is evidenced again, confirming the validity of Eq. (18) also for this case.

The variation of the peak voltage as a function of the resistive load for two rotating frequencies, 0.75 and 2.54 Hz, is presented in Fig. 9(a). It is possible to find an increase of the generated voltage as the resistive load grows. At the same time, larger voltages are found for larger rotating frequencies. In addition, the generated current as a function of the resistive load is shown in Fig. 9(b). In comparison with Fig. 9a, in this case, the opposite behavior is observed. The largest current corresponds to the smallest resistance and the current decreases as the resistance increases. As in the previous case, the current increases as the excitation frequency increases.

We repeated the same experiments for the addition of a mass m to beam#1. The results of these tests show similar values to those presented in Fig. 8 (not presented here for simplicity). The natural frequency at 0 rotation speed drops to 12.57 Hz in this case, which is a little higher than in the previous case. This can be explained by the fact that beam#2 is more flexible than beam#1, thus making the reduction larger due to the addition of mass.

The simple harvesting circuit of Fig. 3 is proposed to capture the accumulated harvested power. A 47 μF electrolytic capacitor C_{rect} was selected for the harvesting circuit as storage device. We used germanium diodes instead of the normal silicon ones in the rectifier bridge in order to minimize voltage drops. Therefore, the capacitor accumulates the rectified DC generated by the REH device as the system rotates. To calculate the average harvested power during a certain period of time, we follow [21], which introduces the following expression for the rectified output power

$$P_{\exp} = \frac{C_{rect}\left(V_{rect1}^2 - V_{rect0}^2\right)}{2\Delta t} \tag{20}$$

This is an approximation for the accumulated harvested power in a capacitor during the interval of time Δt, and V_{rect1} and V_{rect0} are the

Table 1
Material and geometrical parameters of the REH.

Steel (primary beam)		MIDE QP16N		Spring		Aluminum (secondary beam)	
Young's modulus	210 GPa	Young's modulus	67 GPa	Stiffness	560 N/m	Young's modulus	67 GPa
Density	7850 kg/m^3	Density	7800 kg/m^3	Length	52 mm	Density	2700 kg/m^3
L_1	45.97 mm	Piezoelectric constant d_{31}	−210 pm/V	Diameter	13 mm	L_3	89.7 mm
L_2	24.06 mm	Capacitance	125 nF			b_3	18.3 mm
b_2	23.2 mm					t_3	0.5 mm
t_2	0.5 mm					M_2	31 gr
M_1	24 gr					r_2	30 mm
r_1	82 mm						

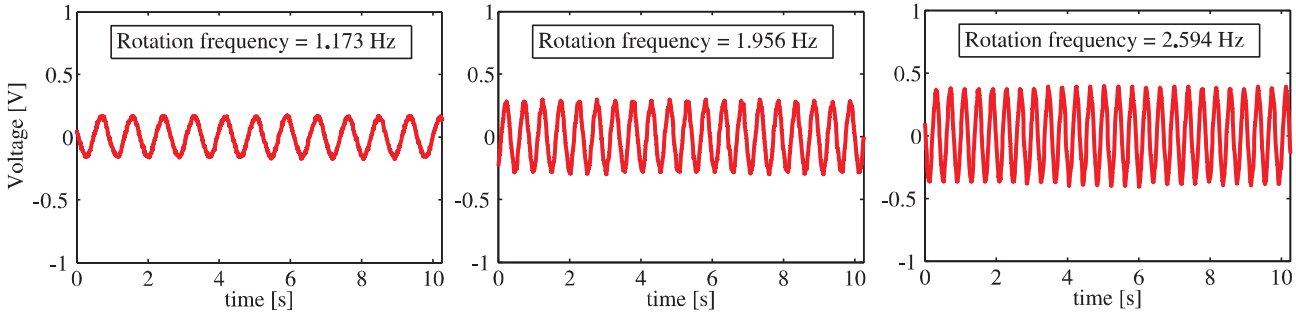

Fig. 5. Voltage output for different rotating frequencies of the proposed REH.

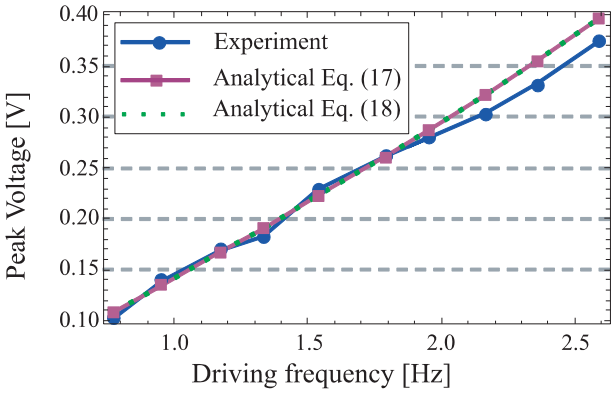

Fig. 6. Voltage output versus rotating frequencies. Experimental, analytical (Eq. (17)) and linear approximation (Eq. (18)).

Table 2
Numerical and experimental values for the cases shown in Fig. 6. (Numerical values of Eqs. (17) and (18) are identical up to the considered precision).

Ω [Hz]		Experiment	Analytical	
rpm	Hz		Eqs. (17) and (18)	Open circuit
46	0.77	0.103	0.109	16.893
57	0.95	0.139	0.135	16.957
70	1.17	0.169	0.167	17.055
80	1.33	0.183	0.191	17.138
92	1.54	0.229	0.223	17.267
107	1.79	0.262	0.262	17.451
117	1.96	0.280	0.288	17.586
130	2.17	0.304	0.323	17.782
141	2.36	0.332	0.356	17.984
155	2.59	0.375	0.397	18.259

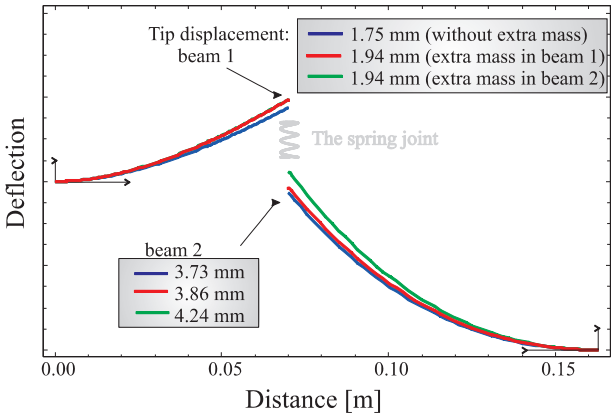

Fig. 7. Influence of the extra mass on the first mode shape and tip displacements of beam #1 and beam#2 for a speed rotation of 155 rpm.

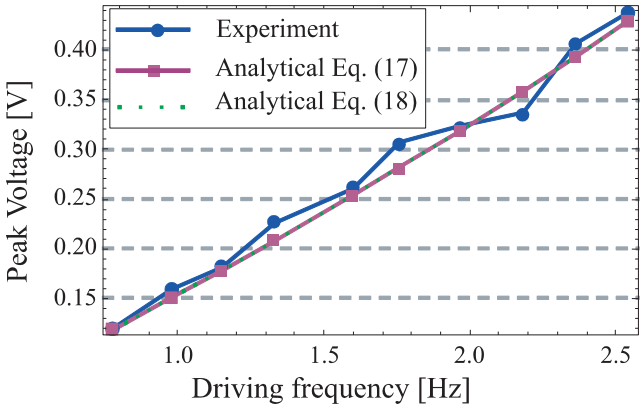

Fig. 8. Voltage output versus rotating frequencies. Experimental, analytical (Eq. (17)) and linear approximation (Eq. (18)) with an extra mass at beam#2.

Table 3
Numerical and experimental values for the cases shown in Fig. 8. (Numerical values of Eqs. (17) and (18) are identical up the considered precision).

Ω [Hz]		Experiment	Analytical	
rpm	Hz		Eqs. (17) and (18)	Open circuit
46	0.77	0.120	0.119	18.510
59	0.98	0.159	0.151	18.612
69	1.15	0.182	0.178	18.714
80	1.33	0.226	0.209	18.847
96	1.60	0.261	0.254	19.082
106	1.76	0.306	0.282	19.244
118	1.97	0.323	0.319	19.481
131	2.18	0.336	0.358	19.763
141	2.35	0.407	0.393	20.029
152	2.53	0.438	0.430	20.327

storage voltages at the start and end of the charging process. In the experiments, we use the same Arduino board with Bluetooth connection to register V_{rect} and set $V_{rect1} = 5V$ and $V_{rect0} = 4V$. The time interval Δt is computed from these collected data in a PC. Fig. 10 shows the output power for the case where a mass m is added to the beam#2. We selected this case, because it represents a larger voltage generation compared to the one without the addition of mass.

From the results, a minimum harnessed power of 25.96 μW for a rotating frequency of 0.77 Hz (46.2 rpm) and a maximum harvested power of 104.74 μW for a rotating frequency of 2.54 Hz (155.4 rpm) can be observed. The consideration of the conversion efficiency, which is a fundamental parameter in order to compare energy harvesters, is also shown in the inset of Fig. 10. The calculation has been performed following a procedure borrowed from Shu and Lien [27] who define efficiency as the rate of the time-averaged output power and the time-averaged power done by the external force. The results show a growing efficiency as the output power grows, with values larger than 0.8. These

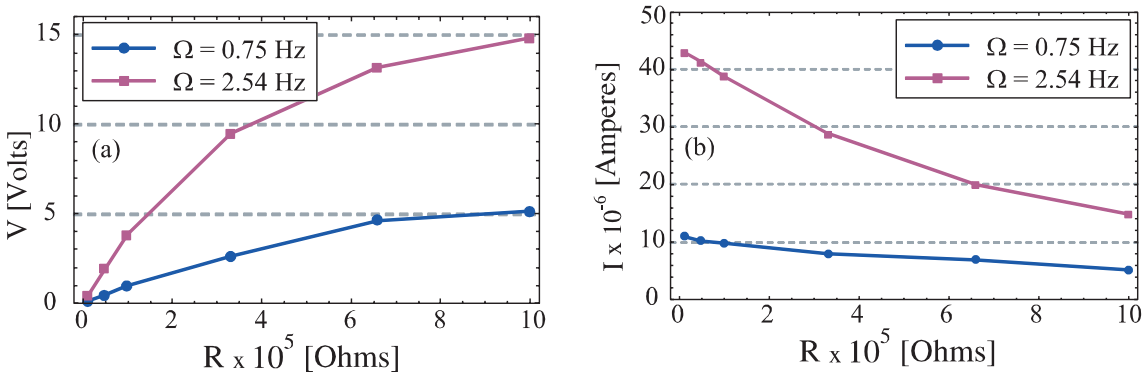

Fig. 9. (a) Output voltage and (b) current as a function of resistive load for the case of adding an extra mass to beam #2, for rotating frequency: 0.75 Hz, 2.54 Hz.

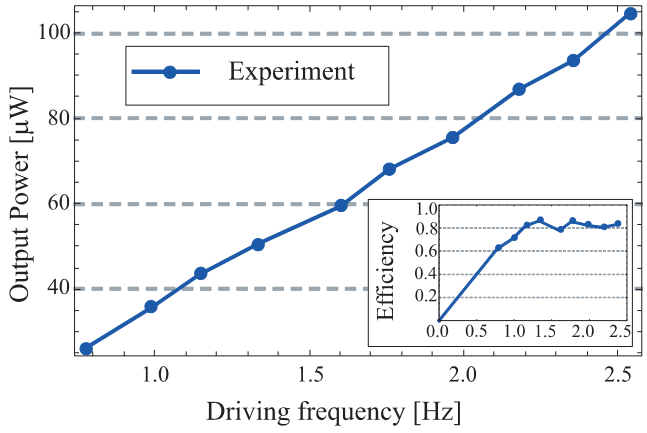

Fig. 10. Experimental power output in the storage device (capacitor) as a function of rotating frequency for the case where an extra mass is added to beam #2. Efficiency as a function of rotating frequency (inset).

values demonstrates a very large efficiency and they are comparable to those obtained in [27] for the case of strong electromechanical coupling and low damping.

Even though the conversion efficiency is high, the absolute values of the output power may not represent a large power compared with previous reports (see for example [14]). However, it is possible to improve the harvested energy by applying further modifications to some of the physical parameters suggested before. Moreover, the introduction of other adaptive harvesting schemes will also increase the harvested power [28]. We must point out that a minimum power requirement of 20 μW is needed to ensure enough power to feed a wireless transmitter circuit [14]. For this reason, our proposed system can be considered as a good candidate to power an autonomous structural monitoring system for 30 kW aero generators working at 50–150 rpm.

It is important to note that a previous work by Guan and Liao [21] reported a REH generator with a power density of 2.29–22.77 μW/cm^3 in the frequency interval 7–13.5 Hz. Our system, on the other hand, collected a power density between of 2.27–9.18 μW/cm^3 in a lower frequency interval (0.77–2.59 Hz), thus presenting a very appropriate solution for very low frequency rotational environments, for example wind turbines. Additionally, this power density can be easily increased with a bimorph piezoelectric sheet, without strongly altering the structural properties of the device. In this sense, our quantitative results would be comparable to those of previous reports [21] where a bimorph piezoelectric beam is used.

5. Conclusions

This paper presents an alternative to simple cantilever piezoelectric beams attached to a rotating hub for scavenging energy. The device is developed to power wireless autonomous monitoring systems of wind turbines of 30 kW, whose operating bandwidth is defined by the rotation speeds of the aerogenerator, ranging 50–150 rpm. The REH comprises two flexible beams and two heavy masses joined by a spring, with a piezoelectric sheet mounted on one of the beams. Based on the Lagrangian formulation, an analytical framework is developed to describe the motion of the system and the voltage output as a function of rotation speed. Special attention was paid to model the tip masses as heavy masses with their rotary inertia included in the kinetic energy. A prototype REH device was implemented to test the validity of the theoretical assumptions. The following conclusions can be drawn for the analyzed cases:

- The results show very good agreement between the theoretical predictions and the experimental tests.
- A linear dependence of voltage output on rotational frequency is observed and predicted by means of a simple analytical expression.
- By proposing a versatile geometrical configuration with two elastic beams and two heavy masses joined by a spring, it is possible to study the effect of an extra mass at various positions of the REH.
- Adding an extra mass to one of the beams, yields nontrivial results. Although it reduces the first bending frequency and increases the harvested energy of the REH device, the tip beam displacements were the same, regardless of the beam where the mass is added. As a result, the same output power is obtained for the two cases.
- The generated DC power (26–105 μW) in the proposed bandwidth (50–150 rpm) enough to feed low-power wireless transmitters for the required monitoring application.

In future works, the following items will be considered.

- A nonlinear spring will be added to replace the linear spring to increase the bandwidth of the REH system.
- A multifrequency excitation will be added to simulate additional periodic excitations.
- Elastic boundary conditions will be introduced to connect the REH device to the frame of the system and thus decrease the first bending frequency.
- An additional piezoelectric sheet will be added to the other beam of the REH device to increase the harvested energy.
- Various durability tests will be performed to study the lifetime of the proposed REH system.

Acknowledgments

The authors wish to thank CONICET (PIP N°: 11220120100346), UNS, UTN FRBB and ANPCyT under grant PICT 2013-2065 for their financial support.

Appendix A

The solutions for the three-beam section are given by:

$$\phi_{i,1}(x_1) = C_1\sin\beta_{i,1}x_1 + C_2\cos\beta_{i,1}x_1 + C_3\sinh\beta_{i,1}x_1 + C_4\cosh\beta_{i,1}x_1,$$
$$\phi_{i,2}(x_2) = C_5\sin\beta_{i,2}x_2 + C_6\cos\beta_{i,2}x_2 + C_7\sinh\beta_{i,2}x_2 + C_8\cosh\beta_{i,2}x_2,$$
$$\phi_{i,3}(x_3) = C_9\sin\beta_{i,3}x_3 + C_{10}\cos\beta_{i,3}x_3 + C_{11}\sinh\beta_{i,3}x_3 + C_{12}\cosh\beta_{i,3}x_3,$$

where, $x_2 = x - L_1$, $x_3 = x - (L_1 + L_2)$, C_j (j = 1–12) are constants to be determined, while

$$\beta_{i,1} = \left(\frac{\omega_i^2\rho A_1}{EI_1}\right)^{\frac{1}{4}}, \quad \beta_{i,2} = \left(\frac{\omega_i^2\rho A_2}{EI_2}\right)^{\frac{1}{4}}, \quad \beta_{i,3} = \left(\frac{\omega_i^2\rho A_3}{EI_3}\right)^{\frac{1}{4}},$$

The following boundary and compatibility conditions are given as follows:

$$\phi_{i,1}(0) = 0, \phi'_{i,1}(0) = 0$$
$$\phi_{i,1}(L_1) = \phi_{i,2}(0), \phi'_{i,1}(L_1) = \phi'_{i,2}(0), EI_1\phi''_{i,1}(L_1) = EI_2\phi''_{i,2}(0), EI_1\phi'''_{i,1}(L_1) = EI_2\phi'''_{i,2}(0),$$
$$EI_2\phi''_{i,2}(L_2) = (I_{T1} + M_1d_1^2)(\omega^2 + \dot{\theta}^2)\phi'_{i,2}(L_2) + M_1d_1(\omega^2 + \dot{\theta}^2)\phi_{i,2}(L_2),$$
$$EI_2\phi'''_{i,2}(L_2) = k[\phi_{i,2}(L_2) - \phi_{i,3}(0)] - M_1(\omega^2 + \dot{\theta}^2)\phi_{i,2}(L_2) - M_1d_1(\omega^2 + \dot{\theta}^2)\phi_{i,2}(L_2)$$
$$EI_3\phi''_{i,3}(0) = (I_{T2} + M_2d_2^2)(\omega^2 + \dot{\theta}^2)\phi'_{i,3}(0) + M_2d_2(\omega^2 + \dot{\theta}^2)\phi_{i,3}(0),$$
$$EI_3\phi'''_{i,3}(0) = k[\phi_{i,3}(0) - \phi_{i,2}(L_2)] - M_2(\omega^2 + \dot{\theta}^2)\phi_{i,3}(0) - M_2d_2(\omega^2 + \dot{\theta}^2)\phi_{i,3}(0)$$
$$\phi_{i,3}(L_3) = 0, \phi'_{i,3}(L_3) = 0$$

Finally, modal amplitude constant is evaluated from a mass normalization according to:

$$\rho A_1\int_0^{L_1}\phi_{j,1}(x)\phi_{n,1}(x)\mathrm{d}x + \rho A_2\int_{L_1}^{L_1+L_2}\phi_{j,2}(x)\phi_{n,2}(x)\mathrm{d}x + \rho A_3\int_{L_1+L_2}^{L_1+L_2+L_3}\phi_{j,3}(x)\phi_{n,3}(x)\mathrm{d}x +$$
$$\phi_{j,2}(L_1+L_2)M_1\phi_{n,2}(L_1+L_2) + \phi_{j,3}(L_1+L_2)M_2\phi_{n,3}(L_1+L_2) + 2M_1d_1\phi_{j,2}(L_1+L_2)\phi'_{n,2}(L_1+L_2) +$$
$$2M_2d_2\phi_{j,3}(L_1+L_2)\phi'_{n,3}(L_1+L_2) + (I_{T1} + M_1d_1^2)\phi'_{j,2}(L_1+L_2)\phi'_{n,2}(L_1+L_2) +$$
$$(I_{T2} + M_2d_2^2)\phi'_{j,3}(L_1+L_2)\phi'_{n,3}(L_1+L_2) = \begin{cases}0 & \text{for } j \neq n.\\ 1 & \text{for } j = n.\end{cases}$$

where the local coordinates x_2 and x_3 were replaced by the global coordinate x.

Appendix B. Supplementary materials

Supplementary data associated with this article can be found, in the online version, at http://dx.doi.org/10.1016/j.enconman.2017.09.042.

References

[1] Roundy S, Wright PK, Rabaey J. A study of low level vibrations as a power source for wireless sensor nodes. Comput Commun 2013;26:1131–44.
[2] Harb A. Energy harvesting: state of the art. Renew Energy 2011;36:2641–54.
[3] Beeby SP, Tudor MJ, White NM. Energy harvesting vibration sources for microsystems applications. Meas Sci Technol 2006;17:175–95.
[4] Mitcheson PD, Yeatman EM, Rao GK, Holmes AS, Green TC. Energy harvesting from human and machine motion for wireless electronic devices. Proc IEEE 2008;96:1457–86.
[5] Yang Z, Zu J. High-efficiency compressive-mode energy harvester enhanced by a multi-stage force amplification mechanism. Energy Convers Manage 2014;88:829–33.
[6] Fan K, Chang J, Chao F, Pedrycz W. Design and development of a multipurpose piezoelectric energy harvester. Energy Convers Manage 2015;96:430–9.
[7] Wang Y, Tang B, Zhang S. Organic, cross-linking, and shape-stabilized solar thermal energy storage materials: a reversible phase transition driven by broadband visible light. Appl Energy 2014;113:59–66.
[8] Sun DM, Wang K, Zhang XJ, Guo YN, Xu Y, Qiu LM. A traveling-wave thermoacoustic electric generator with a variable electric R-C load. Appl Energy 2013;106:377–82.
[9] Askari H, Asadi E, Saadatnia Z, Khajepour A, Behra Khamesee M, Zu J. A hybridized electromagnetic-triboelectric self-powered sensor for traffic monitoring: concept, modelling, and optimization. Nano Energy 2017;32:105–16.
[10] Leland ES, Wright PK. Resonance tuning of piezoelectric vibration energy scavenging generator using compressive axial preload. Smart Mater Struct 2006;15:1413–20.
[11] Eichhorn C, Goldschmidtboeing F, Woias P. Bidirectional frequency tuning of a piezoelectric energy converter based on a cantilever beam. J Micromech Microeng 2009;19:094006–94012.
[12] Manla G, White NM, Tudor J. Harvesting energy from vehicle wheels. Solid-State Sensors, Actuators and Microsystems Conf., 2009. TRANSDUCERS 2009:1389-92.
[13] Zheng Q, Tu H, Agee A and Xu Y. Vibration energy harvesting device based on asymmetric air-spaced cantilevers for tire pressure monitoring system. PowerMEMS (Washington, DC); 2009. p. 403–6.
[14] Roundy S, Tola J. Energy harvester for rotating environments using offset pendulum and nonlinear dynamics. Smart Mater Struct 2014;23:105004–15.
[15] Manla G, White NM, Tudor MJ. Numerical model of a non-contact piezoelectric energy harvester for rotating objects. IEEE Sens J 2009;12:1785–93.
[16] Gu L, Livermore C. Passive self-tuning energy harvester for extracting energy from rotational motion. Appl Phys Lett 2010;97:081904–81908.
[17] Gu L, Livermore C. Compact passively self-tuning energy harvesting for rotating applications. Smart Mater Struct 2012;21:015002–11.
[18] Khameneifar F, Moallem M, Arzanpour S. Modeling and analysis of a piezoelectric energy scavenger for rotary motion applications. J Vib Acoust 2011;133:011005.
[19] Khameneifar F, Arzanpour S, Moallem M. A piezoelectric energy harvester for rotary motion applications: design and experiments. IEEE Trans Mech 2013;18:1527–34.
[20] Hsu JC, Tseng CT, Chen YS. Analysis and experiment of self-frequency-tuning piezoelectric energy harvesters for rotational motion. Smart Mater Struct 2014;23:075013.
[21] Guan M, Liao WH. Design and analysis of a piezoelectric energy harvester for rotational motion system. Energy Convers Manage 2016;11:239–44.
[22] Cottone F, Vocca H, Gammaitoni L. Nonlinear energy harvesting. Phys Rev Lett 2009;102:080601–5.

[23] Erturk A, Hoffmann J, Inman DJ. A piezo magneto elastic structure for broad band vibration energy harvesting. Appl. Phys. Lett. 2009;94:254102–5.
[24] Ramezanpour R, Nahvi N, Ziaei-Rad S. Electromechanical behavior of a pendulum-based piezoelectric frequency up-converting energy harvester. J Sound Vib 2016;370:280–305.
[25] Younesian D, Askari H, Saadatnia Z, Yazdi MK. Free vibration analysis of strongly nonlinear generalized Duffing oscillators using He's variational approach & homotopy perturbation method. Nonlinear Sci Lett A 2011;2:11–6.
[26] Machado SP, Febbo M, Rubio-Marcos F, Ramajo LA, Castro MS. Evaluation of the performance of a lead-free piezoelectric material for energy harvesting. Smart Mater Struct 2015;24:115011–9.
[27] Shu YC, Lien IC. Efficiency of energy conversion for a piezoelectric power harvesting system. J Micromech Microeng 2006;16:2429–38.
[28] Liang J, Liao WH. Improved design and analysis of self-powered synchronized switch interface circuit for piezoelectric energy harvesting systems. IEEE Trans Ind Electron 2012;59:1950–60.